

# EFFECT OF VARIATION OF SLAG CONTENT ON CHEMICAL, ENGINEERING AND MICROSTRUCTURAL PROPERTIES OF THERMALLY CURED FLY ASH-SLAG BASED GEOPOLYMER COMPOSITES

**Kushal Ghosh\* and Partha Ghosh**

Department of Construction Engineering, Jadavpur University, Kolkata, India

\*E-mail: [kushalghosh100@gmail.com](mailto:kushalghosh100@gmail.com)

---

## ABSTRACT

The microstructure, mechanical properties and reaction products of alkali-activated fly ash-slag geopolymer composites and their interdependence are assessed in this paper. The percentage of ground granulated blast furnace slag has been varied from 10% to 60%. All specimens have been subjected to a curing temperature of 85°C. Phase characterization of the samples have been conducted with the help of XRD analysis which pointed to the fact that the reaction products bore more similarity with the alkali activation of fly ash composites rather than alkali-activated slag composites. The change in the bond formulations of the atoms has been studied by FTIR. FESEM and TGA/DTA analysis have also been done to explain the changing microstructural features of the samples due to the presence of slag. It was observed that the compressive strength and bulk density increased and water absorption, apparent porosity decreased due to the presence of slag up to 30%. The ultrasonic pulse velocity also increases with the increase in slag percentage up to 30%. The flow diameter was also observed to increase, reaching the maximum level of 220 mm for a mix containing 60% slag.

© RASAYAN. All rights reserved

---

## INTRODUCTION

Portland cement is the most widely used binding material in the manufacture of concrete. But the production of one ton of cement produces one ton of greenhouse gas<sup>1</sup>. In order to reduce this large amount of carbon dioxide emission, alternative binding materials such as alkali activated composites or “Geopolymers” are being increasingly used. The name “Geopolymers” was first used by Davidovits to describe a form of an inorganic binder made, using alumina-silicate rich precursors and alkaline solutions. Geopolymerisation usually occurs in four stages e.g dissolution, gelation, solidification, polycondensation and crystallization. These four stages may occur discreetly or simultaneously to form a solid material with superior strength and durability properties in comparison to Portland cement<sup>2-3</sup>. Fly ash and blast furnace slag are the most widely used precursors in the manufacture of alkali-activated composites with a number of studies being conducted in that area<sup>4-9</sup>. Among the two materials fly ash is the more popular choice because it is more abundantly available and its disposal is a problem. Safe and effective disposal of effluent, sludge and other waste products such as fly ash formed due to coal combustion is a major challenge being faced by the industries today. In the year 2015, the amount of the fly ash produced in India was 176.74 million tons and fly ash utilization was 107.77 million tons<sup>10</sup>. Most of the unutilized ash is disposed in landfills at suitable sites<sup>11-12</sup>. Landfilling is not a favorable option as it increases the total cost of running foundries and also has its own set of regulatory approvals<sup>13</sup>. Groundwater contamination due to toxic metals present in landfills also is of critical concern. Fly ash has reactive silica and also possesses good acid neutralization properties.<sup>14-15</sup> Fly ash has a comparatively low reactivity and needs a high alkaline liquid to binder ratio to achieve good results. But studies performed on blended precursors have been seen to yield more favorable results in terms of strength, workability and durability than composites manufactured from sole precursors<sup>16-17</sup>. Addition of slag, a material already being used in the construction industry in various forms<sup>18-20</sup> has been seen to vastly improve the reactivity of the

geopolymer mix leading to better workability and high early strength. Most of the experimental programs involved water curing at ambient temperature. The geopolymerisation of fly ash requires thermal curing of about 70-85°C to form proper alumina-silicate reaction products<sup>21-22</sup>. This is partly the reason that the studies of Ismail et al.<sup>24</sup>, J. Oh et al.<sup>25</sup> have reported that the reaction products of the alkali-activated fly ash-slag geopolymers bore more resemblance to end products of alkali-activated slag composites. Addition of alkaline solution to slag leads to the disintegration of calcium and formation of aluminum precipitates which leads to the formation of a C-A-S-H type gel<sup>24-26</sup>. This gel functions as the major binding agent contributing to the increased level of mechanical strength, decreased the level of porosity and high durability. Geopolymerisation of fly ash leads to the formation of a cation activated alumina-silicate gel i.e. a sodium alumina-silicate gel N-A-S-H<sup>25-26</sup>. Alkali activation of a blended precursor containing slag generally leads to the formation of a hybrid binder system comprising of both C-A-S-H and N-A-S-H gels. The nature of the cross-linkage has been found to depend upon the chemical composition of the precursors and the percentage of the alkaline activator solution. Lloyd<sup>27</sup>, suggested that addition of slag produced C-S-H type reaction products with interlinked aluminum ions depending upon its availability. The impact of slag substitution in fly ash geopolymers and its resultant effect on reaction kinetics was studied by Kumar et al. and they found that the C-S-H gel forms a major portion of the reaction products along with alumina-silicate gels. This concurrent existence of both the gels leads to high early setting and better mechanical properties<sup>25-28</sup>. Provis et al.<sup>30</sup> via X-ray microtomography data also established the dominant presence of slag based reaction products on a microstructural level. A study conducted on the microstructural aspects of younger age pastes by Yang et al.<sup>31</sup> also established the fact that addition of slag in sodium hydroxide activated fly ash geopolymers has an effect on the reaction mechanism which is one of the major controlling factors behind the formation of the main binding gel products.

Most of the previous studies discussed above-used water curing at ambient temperature as slag particles do not need heat curing to reach the hardening stage of alkali-activated binder systems. Significantly less number of studies have been done on thermally cured fly ash slag based geopolymer composites. But to enable the fly ash to participate fully in the geopolymerisation process curing at a higher temperature of 70-90°C is needed<sup>21-22</sup>. It has also been reported that the fire and acid resistance<sup>31-33,34</sup> of fly ash based geopolymers is better than slag based composites. Thus to harness the true potential of a fly ash based blended geopolymer one has to ascertain mixing and curing conditions that allow the fly ash to fully take part in the geopolymerisation reaction. Therefore, this study will characterize the changes in the mechanical as well as microstructural properties of a thermally cured alkali activated fly ash-slag blended geopolymer composite using data regarding compressive strength, water absorption, apparent porosity, bulk density, ultrasonic pulse velocity, XRD, SEM-EDAX, FTIR and TGA/DTA analysis.

## EXPERIMENTAL

### Materials and Sample Preparation

The geopolymer precursors used in this investigation were a fly ash, Class F according to ASTM C 618, from Kolaghat thermal power plant, West Bengal, India, and a ground granulated blast furnace slag supplied by Durgapur Steel plant, West Bengal, India. The oxide compositions of the precursors are given in Table 1. The alkali activator was prepared by dissolution of sodium hydroxide pellets (Merck) in water and then adding sodium silicate (49.1 wt.% SiO<sub>2</sub> and 50.9 wt.% Na<sub>2</sub>O, supplied by Loba Chemicals.) in the mix. The mixture of sodium hydroxide and sodium silicate solution was then permitted to cool to room temperature before being used for the preparation of specimens. The activator doses used were 8 wt.% by total mass of precursor as described in Table 2. Water/binder ratio of 0.38 was used in the preparation of the mix specimens. For making fly ash/slag paste specimens, the fly ash, blast furnace slag and activating solution in desired proportion were first mixed together for 5 to 7 min in a Hobart Mixer to get a homogeneous paste. The flow diameter of the fresh paste was measured on a miniature flow table and then the paste was poured into 50 mm×50 mm×50 mm steel moulds and vibrated for 2 min on a vibrating table to remove any entrapped air. After vibration, the specimens were kept at room temperature

for 4 hours, after which it was kept in an oven and heat cured at 85 °C for 48 hours. After that the samples were taken out and air cured till the time of testing. The tests were conducted at the age of 7 days.

Table-1: Chemical analysis by XRF (%) of the solid binder precursors. LOI is a loss on ignition at 1000 LC

Oxide (wt.%)	SiO <sub>2</sub>	Al <sub>2</sub> O <sub>3</sub>	Fe <sub>2</sub> O <sub>3</sub>	CaO	MgO	SO <sub>3</sub>	Na <sub>2</sub> O	K <sub>2</sub> O	LOI	Others
Fly ash	65.81	22.17	3.23	1.24	1.01	0.47	0.16	2.62	1.57	1.72
Slag	37.25	10.24	1.1	42.17	3.82	2.13	0.19	.66	0.81	1.63

Table-2: Mix proportions of the alkali-activated slag/fly ash blends

Source material ratio ( wt.% fly ash / wt.% slag)	Sodium Metasilicate (Activator) dose relative to total fly ash +slag content (wt.%)	Sodium hydroxide (Activator) dose relative to total fly ash +slag content (wt.%)
100-0	8	8
90-10	8	8
85-15	8	8
70-30	8	8
50-50	8	8
40-60	8	8

### Analytical Techniques

The microstructural and chemical analysis was performed on paste samples after an age of 7 days from the date of casting. X-ray diffraction (XRD) using a Rigaku Miniplex Ultima III instrument, scanning from 10° to 80° 2θ, with a 0.02° step size and 2 s/step count time.

Fourier transform infrared (FTIR) spectroscopy, using the KBr pellet method in a Bruker Tensor 27 spectrometer, scanning 32 times from 4000 to 400 cm<sup>-1</sup> at 4 cm<sup>-1</sup> resolution.

Thermogravimetry (TG), in a TA Instruments SDT Q600. Samples were crushed, transferred immediately to an alumina crucible, held under isothermal conditions for 60 min at 40 LC to equilibrate, and then heated 40–1000 LC at 10 LC/min in a nitrogen environment at 200 mL/min purge rate. Field electron scanning electron microscopy (FESEM) with energy dispersive X-ray (EDX) analysis, at an accelerating voltage of 10-20 kV using a (JEOL JSM-6700F) instrument. Compressive strength determination was done on a digital compression testing machine. Ultrasonic Pulse velocity test was done with a Proseq Pundit Lab ultrasonic instrument.

## RESULTS AND DISCUSSION

### Compressive Strength

The compressive strength of the mix is seen to increase with the addition of slag content. There is an increase of 19.99% in the compressive strength of the mix 90-10 over mix 100-0. Mix 85-15 reports an increase of 15.97% over the mix 90-10. The mix 70-30 sees an increase of compressive strength of 14.75% over the mix 85-15. But the mix 50-50 and mix 40-60 reports a decrease of -3.428% and -6.33% over mix 70-30 and mix 50-50 respectively. The increase of strength can be attributed to the more reactive nature of slag particles. The formation of C-S-H gel (Calcium Silicate Hydrate), C-A-S-H (Calcium Alumina-silicate Hydrate gel alongside N-A-S-H (Sodium Alumina-silicate Hydrate) gel has been reported to have a positive effect on the mechanical properties of geopolymers.<sup>24-26</sup> Also Puertas, Provis et al have reported in previous studies that the addition of slag leads to high early strength. This seems to be in sync with results of Kumar et al<sup>25</sup> and Li, Zongjin et al<sup>35</sup> who also reported an increase in compressive strength with the addition of slag in fly ash/slag blended composite. Yip et al. also suggested that the increase in the compressive strength could be due to the coexistence of both C-S-H and geopolymeric gel<sup>36-37</sup>. The presence of Ca could also cause degradation of the geopolymeric gel at high pH and excess Ca in the system could lead to the formation of a highly disordered and unstable

geopolymeric gel. Calcium ions can preferentially form (Ca, K)-A-S-H as the pH of the system lowers in the later age<sup>38</sup>. This could be the reason for the degradation of mechanical properties in mix 50-50 and mix 40-60 in the current study. Yip et al. also reported that the presence of Ca could disrupt the three-dimensional ordering of geopolymers. Another study by I. García-Lodeiro et al, however, reports that Ca ion substitution into a geopolymeric gel network may not cause disordering of the structure but can result in changes of chemical composition<sup>38</sup>. Marjanović et al. reported that the increase in the BFS (Blast furnace slag) content led to a lesser water/binder ratio which in turn resulted in greater compressive strength with the 25%FA-75%BFS mix reporting the highest values<sup>39</sup>. Wardhono et al also reported an increase in compressive strength with slag addition with the mix with 50% slag giving the highest strength<sup>40</sup>. Zhang et al reported a decrease in strength value in a fly ash-slag based composite subjected to ambient temperature curing with slag percentage more than 30% which is in agreement with this study<sup>41</sup>. Further discussions about the other engineering properties are done in the following section.

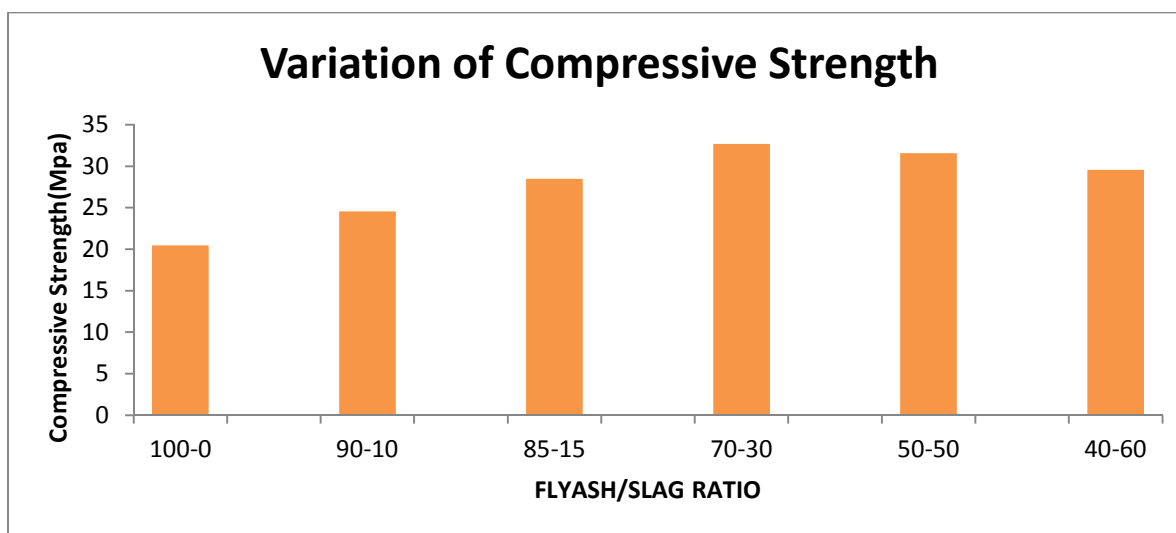


Fig.-1: Effect of variation of slag on compressive strength of the fly ash slag based geopolymer composite

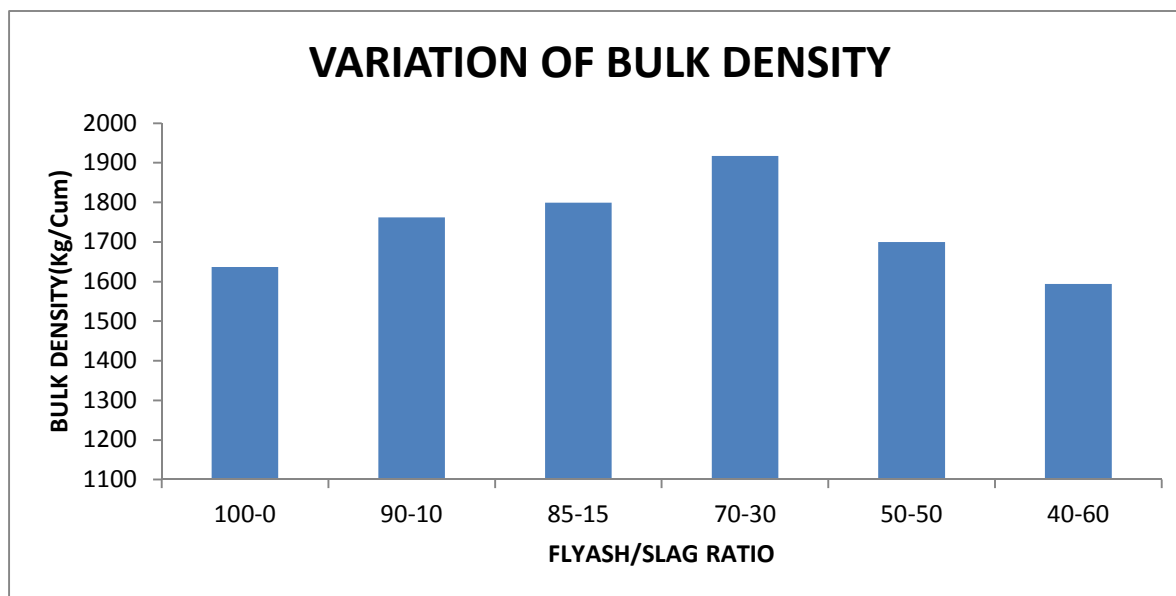


Fig.-2: Effect of variation of slag on the bulk density of fly ash slag based geopolymer composite

### Bulk Density, Water Absorption, Apparent Porosity, Flow diameter and Ultrasonic Pulse Velocity Test Results

The bulk density of the mix 100-0 with fly ash as the sole precursor is seen to have the lowest bulk density value at  $1234.96 \text{ kg/m}^3$ . The value increases to  $1609.66 \text{ kg/m}^3$  for mix 90-10 with 10% addition of slag by weight. The bulk density value for mix 85-15 is a bit higher at  $1633 \text{ kg/m}^3$ . It continues to increase for mix 70-30, with a value of  $1727.44 \text{ kg/m}^3$ . But the mix 50-50 and mix 40-60 show a decrease in bulk density values from the previous mixes at  $1698.42 \text{ kg/m}^3$  and  $1680 \text{ kg/m}^3$  respectively. The results clearly show that the bulk density of the specimens increases with the addition of slag to an optimum level of 30%. This can be explained by the fact that the incorporation of slag which is calcium rich in nature leads to the formation of a denser microstructure which is further confirmed by images as discussed in the section on EDAX/SEM analysis. Though slag has a more reactive nature, which leads to high early strength, the extra charge balancing aluminium ions of fly ash contributes to the long-term nature of the gel structure increasing its rigidity in the process. The above-made arguments about the gel structure of the alkali-activated fly ash slag geopolymers can also be corroborated by the apparent porosity and water absorption results. The apparent porosity of the samples decreases with the increase of slag content up to the optimum level of 30%. The lowest apparent porosity value was found to be lowest at 14.61% for the 70-30 mix and the highest value was found for mix 100-0 at 22.92%.

This can be attributed to the fact that the high reactivity of the slag particles leads to a higher amount of gel formation. The flow diameter has also been observed to increase with slag addition though it did not follow the trend of the other findings and continued to increase up to the mix with the highest amount of slag. The increase of the flow leads to smooth pouring, compaction and casting of the mixes. The mixes with more than 30% slag did not need mechanical vibration. Also, the spherical nature of the fly ash particles leads to the formation of a dense microstructure with a lesser amount of pores.

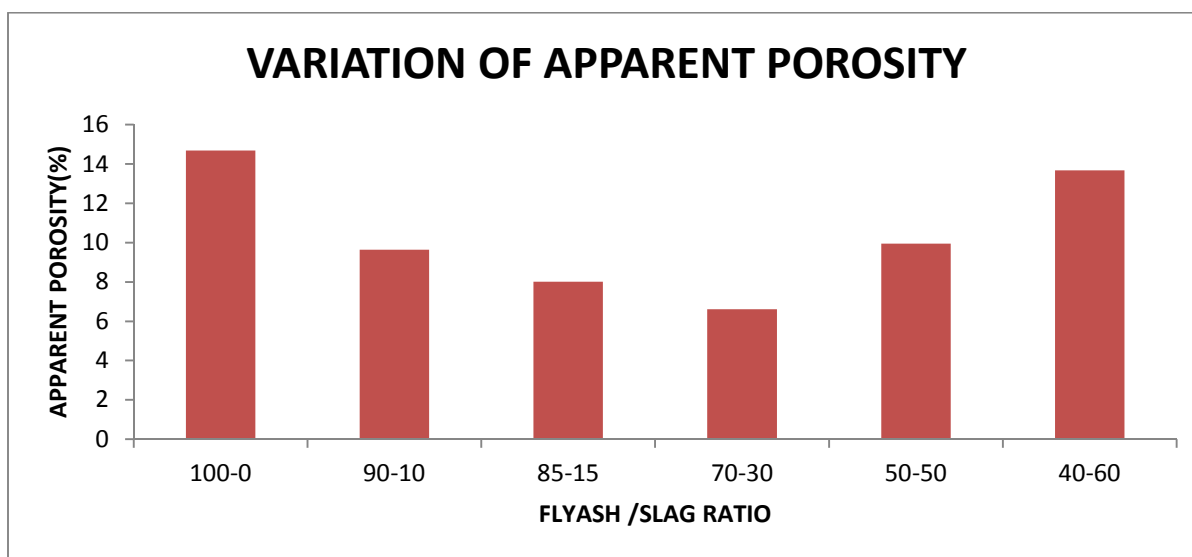


Fig.-3: Effect of variation of slag on the apparent porosity of the fly ash slag based geopolymer composite

The ultrasonic pulse velocity (UPV) data also points to this fact. The UPV values have also been found to increase with the higher slag percentage up to the mix 70-30. The UPV values of the mix 70-30 were the maximum and the phenomenon is in accordance with previous studies involving the microstructure of fly ash-slag blends where it has been reported that a major amount of gel formation involves cross-linkages C-S-H and N-A-S-H gel leading to the formation of a hybrid, rigid 3D tetrahedral gel network<sup>24</sup>. The dissolution of silicon and aluminum species from fly ash is very slow in general. On addition to slag the dissolution rate increases which contributes to the improvement of the gel network and subsequently the

engineering properties<sup>42</sup>. The changes in gel network can be further explained with the XRD, FTIR, FESEM/EDAX analysis discussed in the following sections.

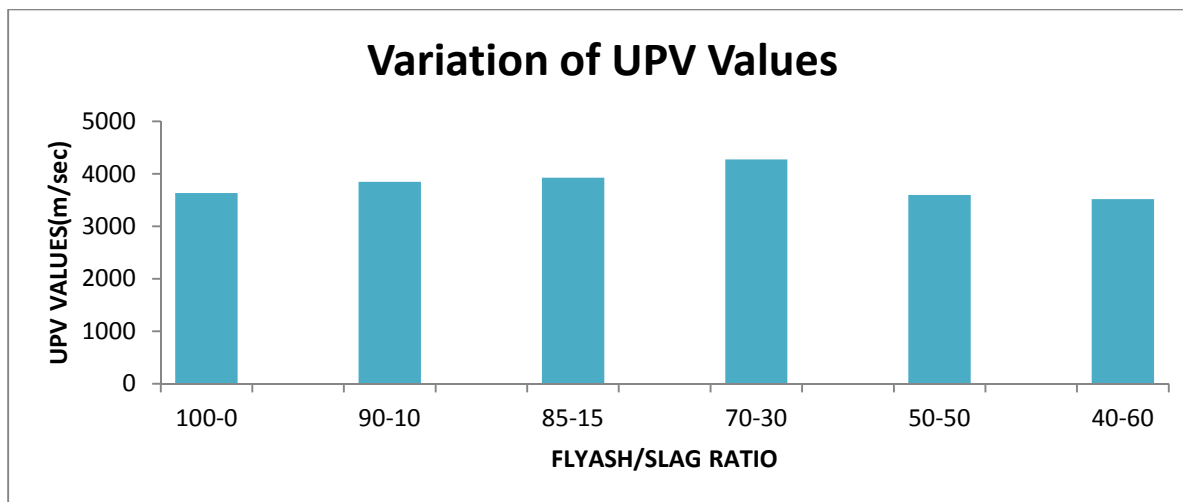


Fig.-4: Effect of variation of slag on ultrasonic pulse velocity values of the fly ash slag based geopolymer composite

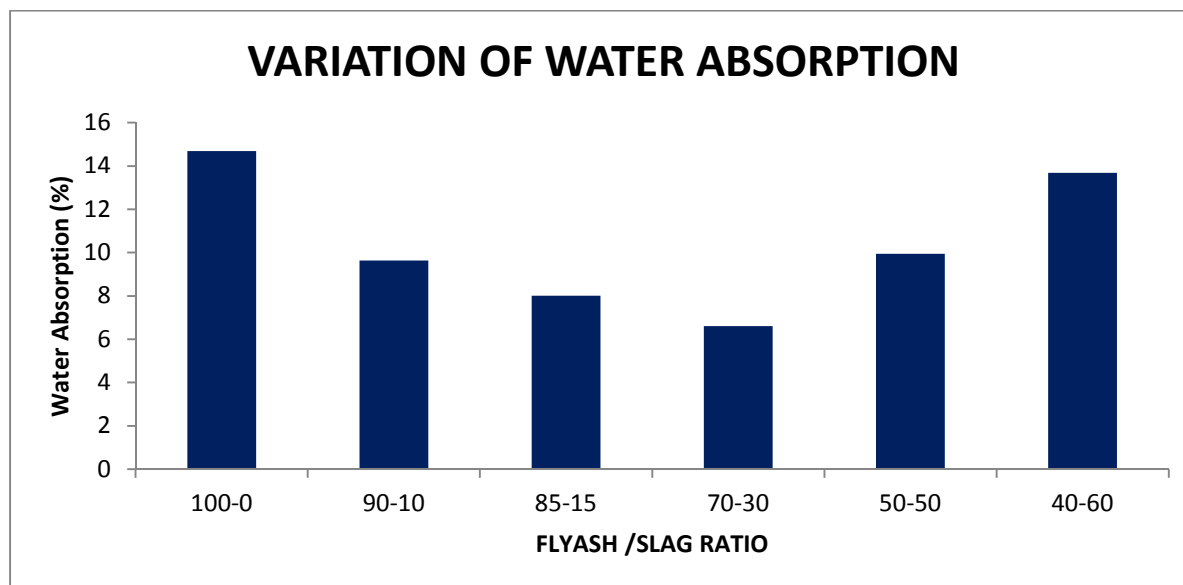


Fig.-5: Effect of variation of slag on water absorption values of the fly ash slag based geopolymer composite

### X-Ray Diffraction Analysis

X-ray diffraction data of the mix 100-0 shows peaks of mainly quartz and mullite and also compounds which can be termed as N-A-S-H gel which is in tune with other findings associated with alkali activation of fly ash based geopolymers. Identifying alumina-silicate gel accurately is a problem as it is highly amorphous in nature thus we will use the peaks of crystalline quartz, mullite to determine the intensity of alumina-silicate gel. With the addition of slag in the mix 90-10 secondary peaks of calcite and the C-S-H gel is to be seen. These peaks appear along with the primary peaks of quartz and mullite. For the mix 85-15, we can observe the same trend with peaks identified as mullite, quartz, calcite and C-S-H gel. In the mix 70-30 the intensity of the peak due to quartz is less than the mix 85-15. The intensity of the C-S-H gel is greater than in the mix 85-15.

This data can be used to argue that as the slag percentage increases there is an increase in calcium-based compounds which essentially functions as a supplementary gel network to the major binding gel network consisting of alumina-silicate compounds. This is supported by the fact that even though there is an increase in peak intensity of calcium-based compounds the highest peaks are still that of alumina-silicate compounds. This data does not align with the results of other research groups (Kumar et al) who have all reported the gel compounds to be predominantly similar to products of alkali activation of slag. But all of those studies were conducted at room temperature which is not conducive to the geopolymerisation of fly ash. In this study as the curing temperature was set at 85°C, a higher degree of geopolymerisation of the fly ash particles took place. But as the slag content increased to 50% and 60% in mix 50-50 and mix 40-60 the mechanical properties were found to decrease .

Q-Quartz    M-Mullite    C-Calcite  
C-S-H-Calcium Silicate Hydrate  
S-Silimanite

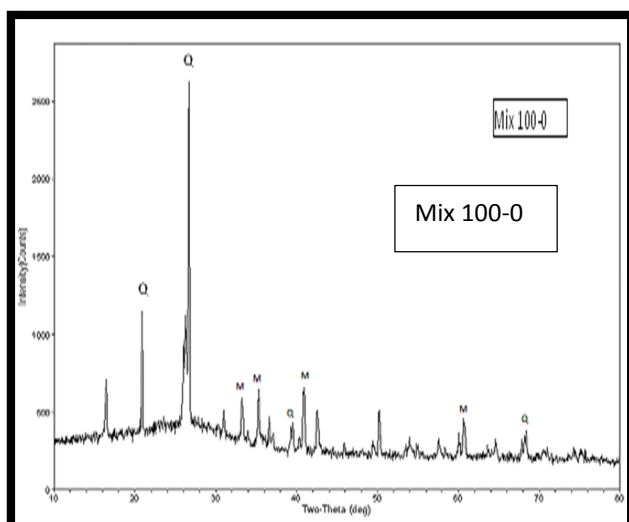


Fig.-6a

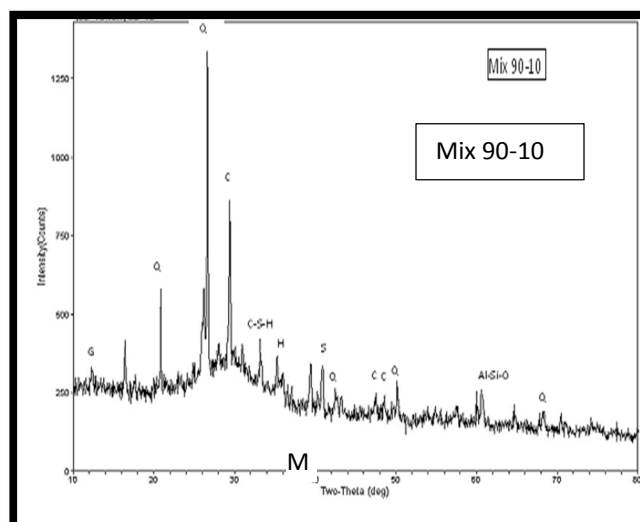


Fig.-6b

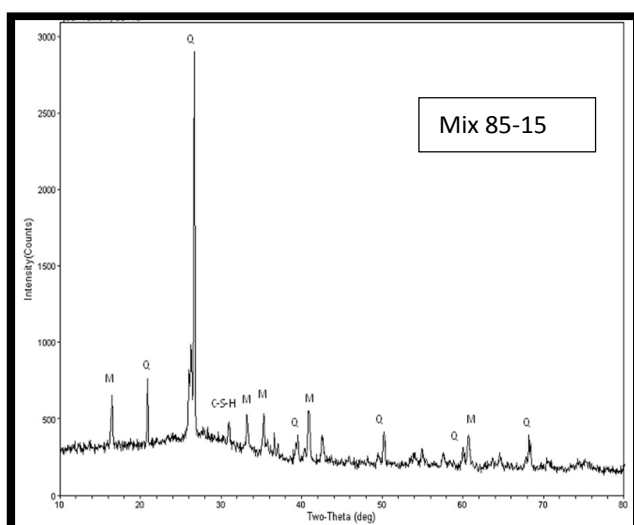


Fig.- 6c

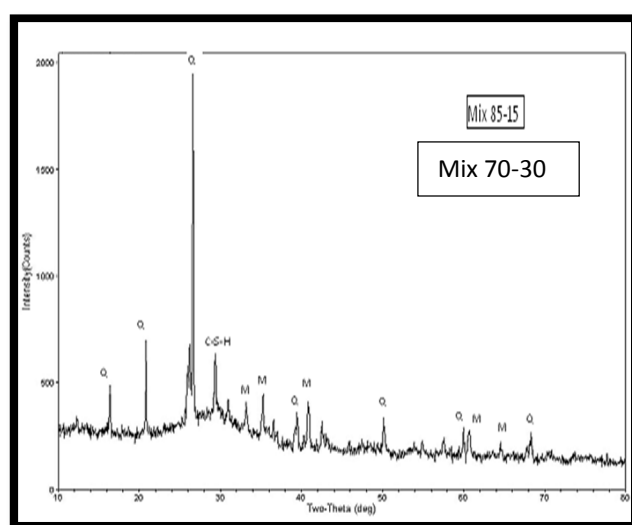


Fig.- 6d

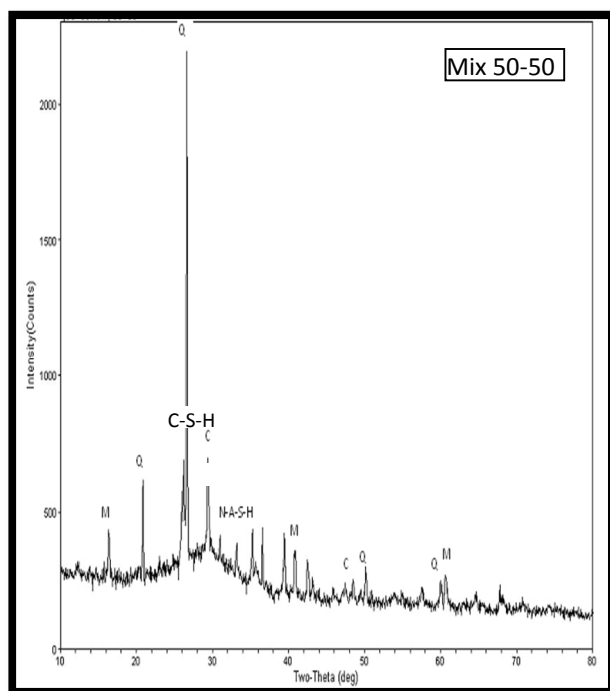


Fig.-6e

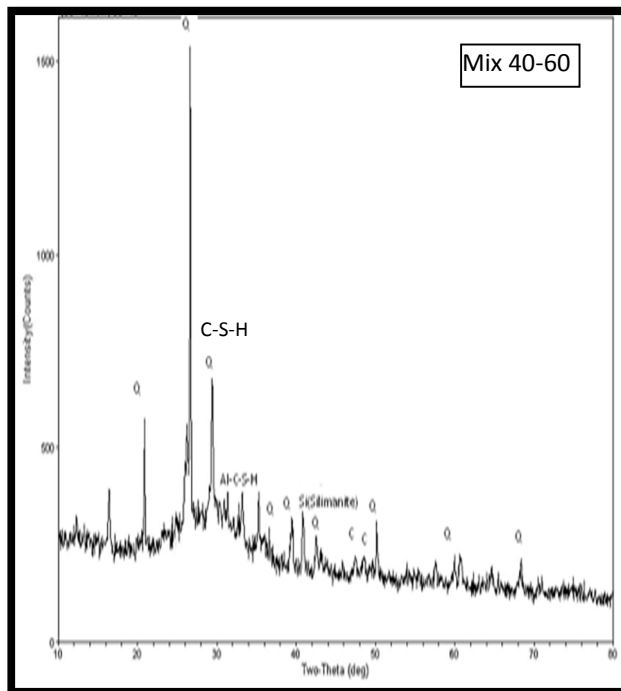


Fig.-6f

Fig.-6(a-f): XRD data for alkali activated slag/fly ash geopolymers as a function of variation of slag

This can be partially explained by the fact that peak intensities for crystalline quartz lessen substantially thus indicating decrease of alumina-silicate gel which was acting as the primary gel network in the previous mixes. Thus a point can be made that the calcium compounds are responsible for enhancing the initial reactivity of the mix but under the effect of high temperature curing it plays the role of a secondary gel network.

### Scanning Electron Microscopy/Energy Dispersive X-Ray Analysis

Looking at the SEM images it can be clearly seen that there has been a gradual change in the microstructure with the addition of slag. The image of mix 100-0 shows the existence of a large number of unreacted circular fly ash particles which does not contribute to the rigidity of the gel network and also hinders its strength gaining nature. The mix 90-10 image also shows a few unreacted fly ash particles but the gel formation is noticeably more.

The fly ash particles have been coated with the gel. The reaction products can be classified as mainly alumina-silicate in nature as the EDAX results are showing much higher peaks of Silica, aluminum than compared to calcium. The mix 85-15 is seen to more amorphous in nature with very few unreacted fly ash particles, the slag particles angular in nature are assumed to fully participate in the gel formation as no angular particle can be seen. The pores present in the structure can also be noticed. The mix 70-30 SEM image shows a structure with a reduction in pores. A few unreacted fly ash particles can still be noticed but these have been covered with reaction products.

In the EDAX analysis, there is a spurt in the peak of calcium which is keeping in tandem with the increase in slag concentration. In the mix 50-50, we can see clearly the separation of phases between the N-A-S-H and C-A-S-H gel. This results in lesser amount of cross-linkages and lessens the cohesive nature of the mix to an extent.

The fly ash particles seem to have participated in the formation of the reaction products. This can also be justified by the fact that there is a lesser amount of fly ash in the mix 50-50 to participate in the



dissolution process and more amount of slag also accelerates the dissolution process. There is also an increase in the percentage of calcium. In the mix 40-60 image, we can see that there are more pore formations than the previous mix which is similar to the findings of apparent porosity of the mixes.

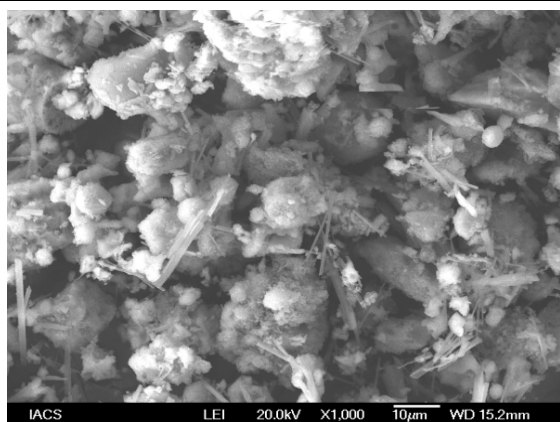


Fig.-7a: 100-0 mix SEM IMAGE

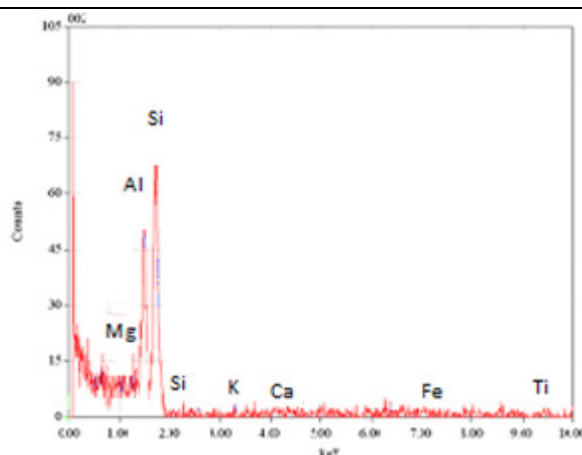


Fig.-8a: 100-0 mix EDAX Results

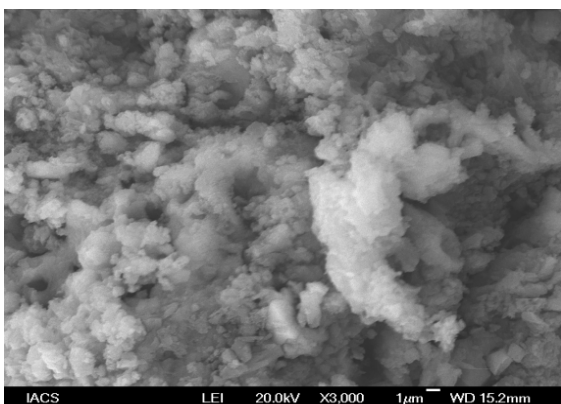


Fig.-7b: 90-10 mix SEM IMAGE

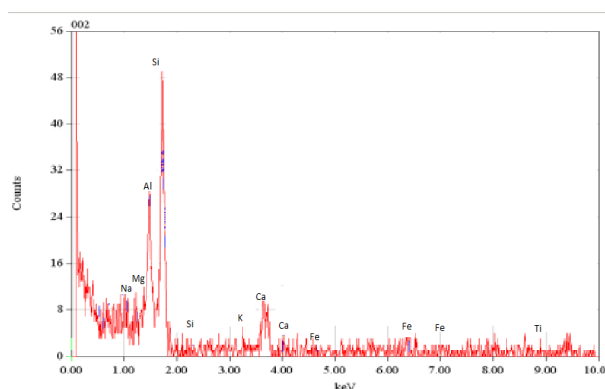


Fig.-8b: 90-10 mix EDAX Results

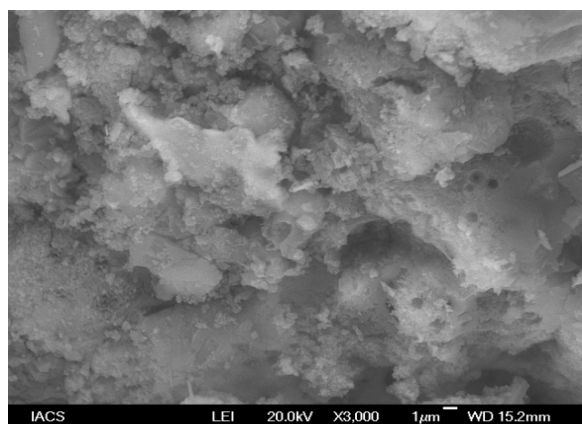


Fig.-7c: 85-15 mix SEM IMAGE

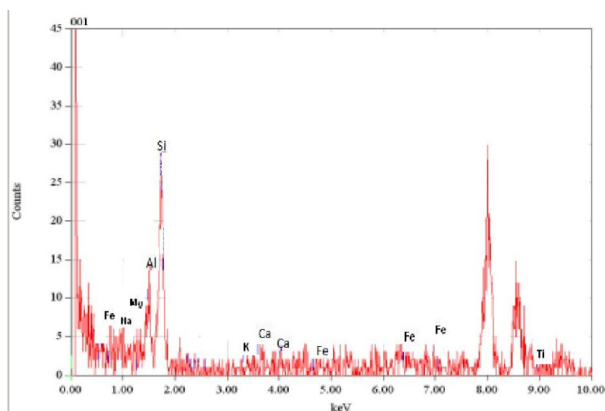


Fig.-8c: 85-15 mix EDAX Results

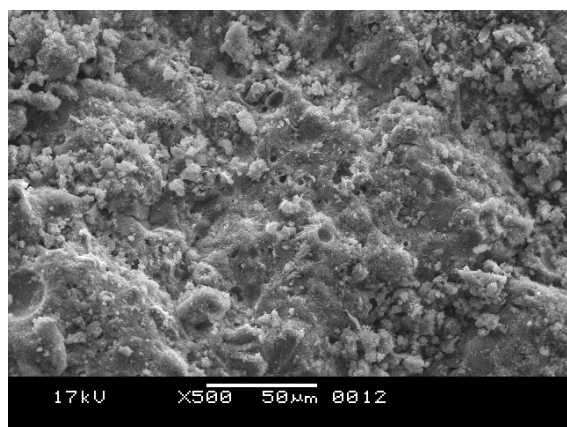


Fig.-7d:70-30 mix SEM IMAGE

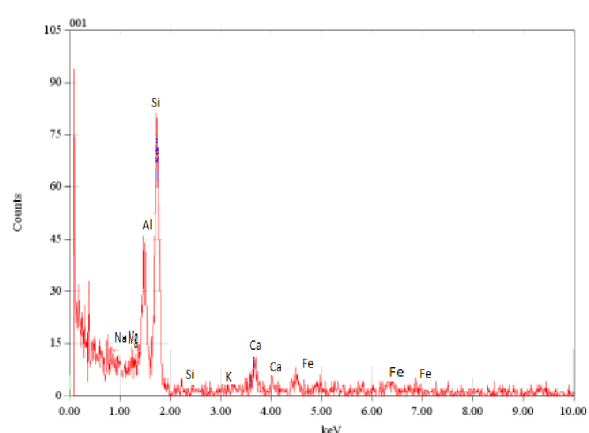


Fig.-8d: 70-30 mix EDAX Results

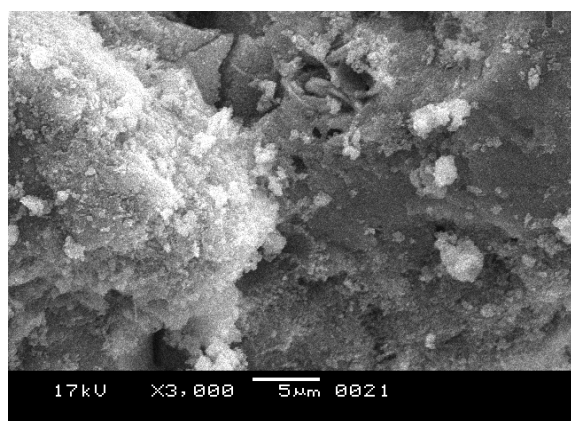


Fig.-7e:50-50 mix SEM IMAGE

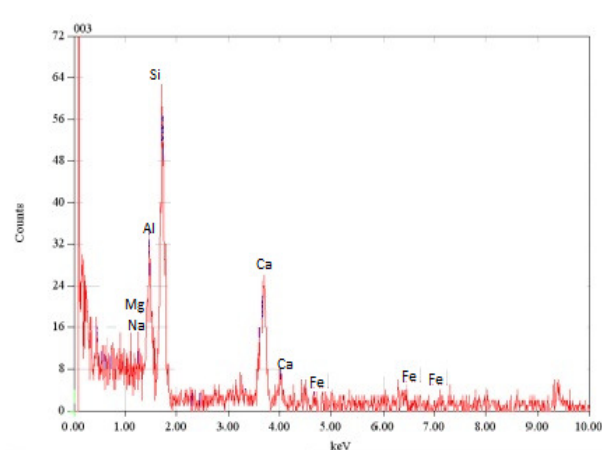


Fig.-8e: 50-50 mix EDAX Results

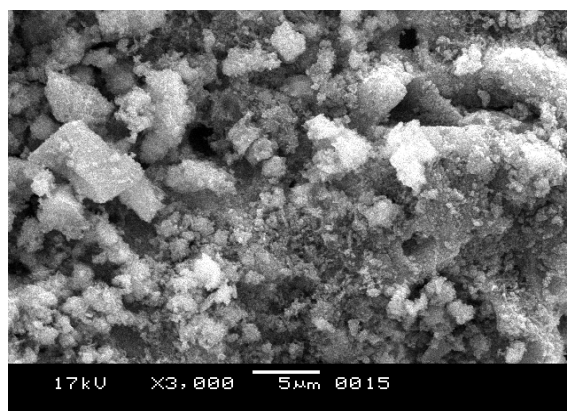


Fig.-7f: 40-60 mix SEM IMAGE

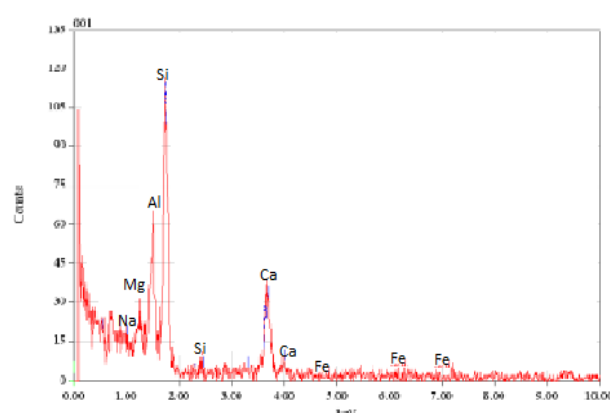


Fig.-8f: 40-60 mix EDAX Results

### FTIR(Fourier Transformation Infrared Spectroscopy) Analysis

The intensity of the broadband between  $3200\text{ cm}^{-1}$  and  $3600\text{ cm}^{-1}$  appears to increase with an increase in the percentage of slag which can be due to the increased early formation of hydration products. Absorption bands from  $1670\text{--}1690\text{ cm}^{-1}$  are assigned to bending vibration O-H group of the

hydrated product also shows an increase in intensity centered at  $1671\text{ cm}^{-1}$ . The wavenumbers associated with Si-O stretching vibrations is seen shifting to lower wavenumbers which can be linked to the fact that the simultaneous activation of fly ash and slag are leading to more crosslinked N-C-A-S-H gel. The band connected with the formation of the main binder gel e.g C-A-S-H gel, N-A-S-H gel in alkali-activated materials has been mainly found in the range of wavenumbers from  $950\text{--}1100\text{ cm}^{-1}$ .<sup>45</sup> here also the main binder gel can be noticed at  $1031\text{ to }1049\text{ cm}^{-1}$  for various mix formulations involving varying degrees of slag. The wavenumbers indicate clearly towards the formation of a hybrid 3-D gel calcium alumina-silicate gel structure.

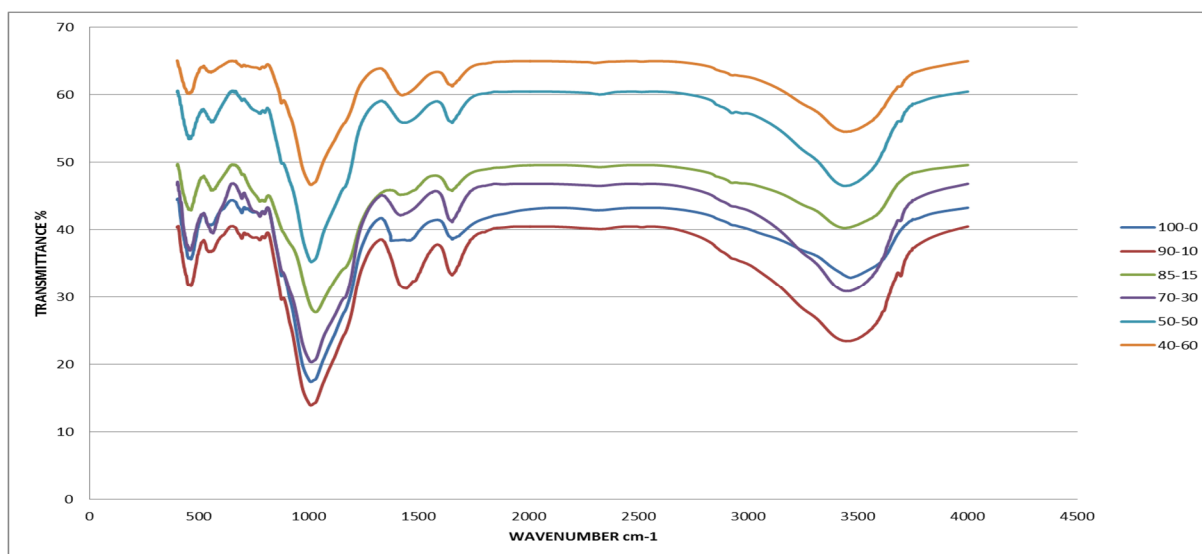


Fig.-9: FTIR spectra of alkali-activated fly ash/slag pastes at different fly ash slag percentages as marked

### TGA/DTG(Thermogravimetric Analysis / Differential Thermogram)

In the above TGA profiles and its relative mass loss percentage, it can be seen that the mass loss percentage at  $15.12\%$  is highest for the mix 40-60. The mix composition with fly ash as the sole precursor had a mass loss of  $8.92\%$  and the mix 90-10 had a mass loss of  $12.68\%$ . Other mix formulations showed a trend of increase of mass loss percentage with increase of slag percentage with Mix ID 85-15, 70-30, 50-50 recording  $13.12\%$ ,  $13.24\%$ ,  $14.95\%$  respectively. Physically bound water in the gel structure is released below the temperature of  $115^\circ\text{C}$ . The samples are showing a decrease in peak temperature values with increase in the percentage of slag. As fly ash particles are spherical and finer in nature less water is trapped in the mix. In previous studies on pore size distribution of fly ash/slag composites, it has been seen that amount of macropores (size  $25\text{nm--}5000\text{nm}$ ) in slag based composites is higher than the percentage present in fly ash based composites<sup>43,44</sup> and as macropores hold a significant amount of free water the slag based composites are reporting peak temperature intensities at lower values. There are also other peak intensities reported between  $550^\circ\text{C}$  to  $600^\circ\text{C}$ .

### CONCLUSION

1. Addition of slag to an optimum level of 30% increases the mechanical properties e.g. compressive strength, bulk density, apparent porosity, water absorption values of a thermally cured fly ash based geopolymer composites. Presence of excess positively charged calcium ions seems to be negatively affecting the gel network. However, the flow diameter of the mix increased almost linearly with the addition of slag.
2. Variation of slag causes changes to the microstructure of the geopolymer composites. Addition of slag leads to the formation of two distinct gel phases e.g N-A-S-H or geopolymeric gel and C-A-S-H gel. XRD analysis also points to the presence of a cross-linked gel phase N-C-A-S-H gel as well. The

N-A-S-H gel primarily functioned as the major load bearing gel phase. In general reaction products bore more resemblance to alkali-activated fly ash geopolymer composites rather than alkali-activated slag based composites. The main reason behind this can be attributed to the use of a higher curing temperature of 85°C which is more conducive for the geopolymerisation of fly ash.

3. TGA/DTA analysis pointed to the fact that presence of a higher percentage of slag leads to the presence of freely available water thus causing greater mass loss of samples with higher slag percentage with the increase of temperature. The sample having fly ash as the sole precursor reported the lowest mass loss by percentage.

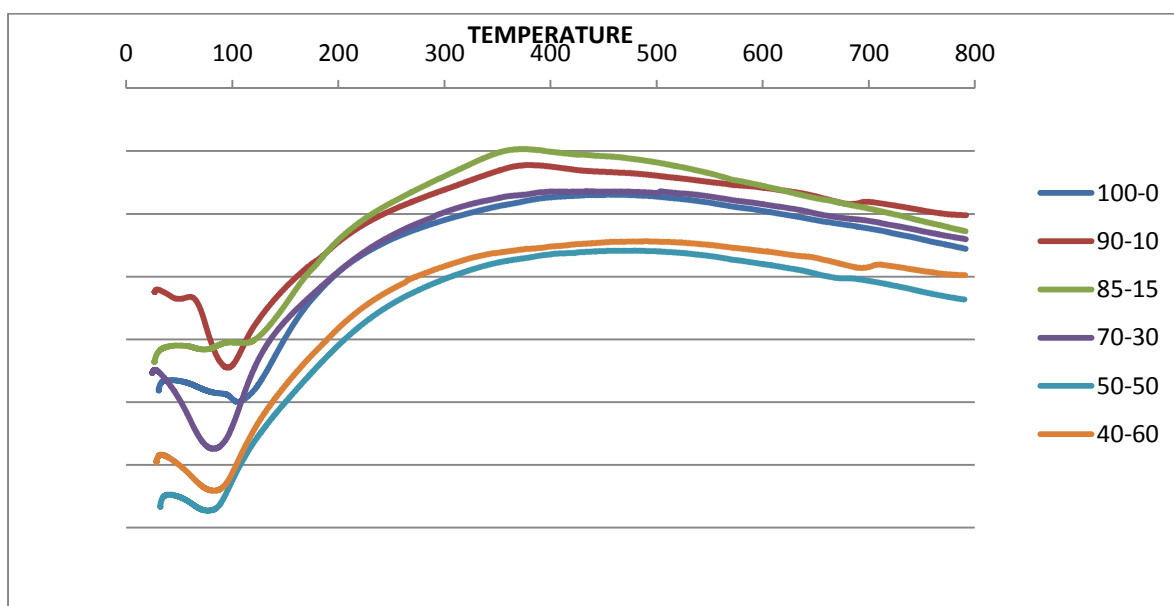


Fig.-10: TGA/DTA Graphical analysis of mass loss peaks of alkali-activated fly ash/slag geopolymer pastes at different fly ash slag percentages as marked

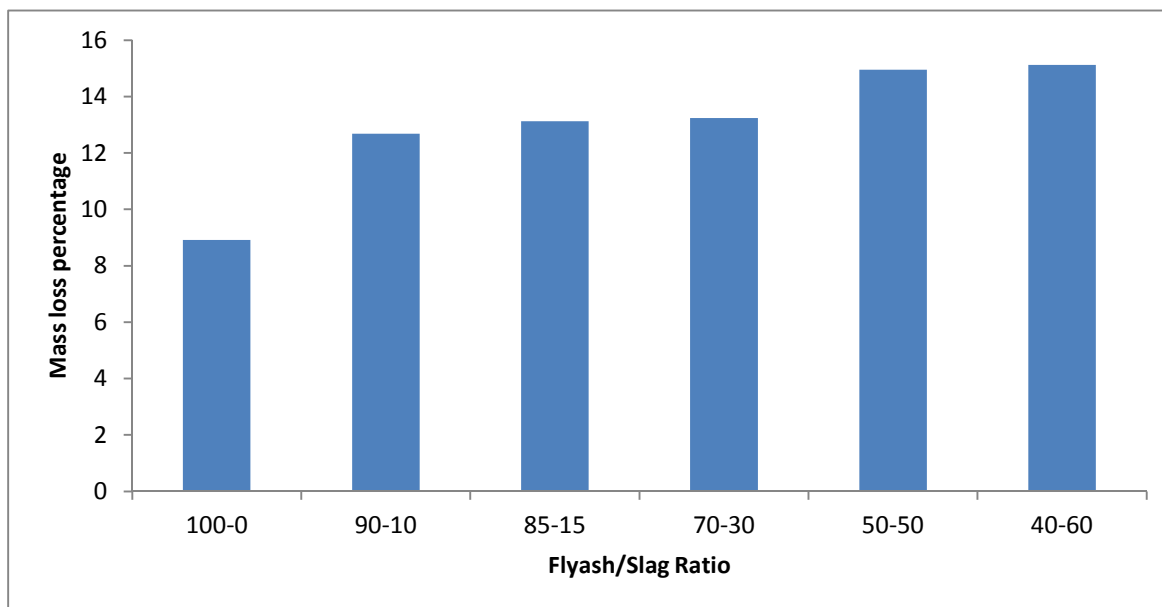


Fig.-11: Mass loss percentage of alkali activated fly ash/slag geopolymer pastes at different fly ash slag percentages as marked



## REFERENCES

1. J. Davidovits, , M. Moukwa, S.L. Sarkar, K. Luke (Eds.), et al., *Ceramic Transactions Cement-based Materials: Present, Future, and Environmental Aspects*, The American Ceramic Society, Westerville, pp. 165 (1993)
2. Jannie S. J. Van Deventer, John L. Provis, Peter Duxson, *Min. Eng*, **29**, 89(2012), DOI: [10.1016/j.mineng.2011.09.009](https://doi.org/10.1016/j.mineng.2011.09.009)
3. Jannie S. J. van Deventer, John L. Provis, Peter Duxson and David G. Brice, *Waste Biomass Valor.*, **1**, 145(2010), DOI: [10.1007/s12649-010-9015-9](https://doi.org/10.1007/s12649-010-9015-9)
4. T. Bakharev, J.G. Sanjayan, Y.B. Cheng, *Cem. Concr. Res.*, **29(1)**, 113(1999), DOI: [10.1016/S0008-8846\(98\)00170-7](https://doi.org/10.1016/S0008-8846(98)00170-7)
5. J. G. S. VanJaarsveld, J. S. J. van Deventer, *Ind. Eng. Chem. Res.*, **38**, 3932(1999), DOI: [10.1021/ie980804b](https://doi.org/10.1021/ie980804b)
6. D. M. Roy. *Cem.Concr.Res.*, **29(2)**, 249( 1999), DOI: [10.1021/ie980804b](https://doi.org/10.1021/ie980804b)
7. A. Palomo, M. W. Grutzeck, M. T. Blanco, *Cem. Concr. Res.*, **29(8)**, 1323(1999), DOI: [10.1016/S0008-8846\(98\)00243-9](https://doi.org/10.1016/S0008-8846(98)00243-9)
8. A. Gruskovnjak , B. Lothenbach , L. Holzer , R. Figi , F. Winnefeld , *Adv. Cem. Res.*, **18(3)**, 119( 2006)
9. Sindhunata, J. L. Provis, G. C Lukey, H. Xu , J. S. J. Van Deventer, *Ind. Eng. Chem. Res.*, **47(9)**, 2991(2008), DOI: [10.1021/ie0707671](https://doi.org/10.1021/ie0707671)
10. D. Hardjito, S. E. Wallah, D.M.J.Sumajouw, B.V. Rangan, *ACI Mater J* **101:1**(2004)
11. C.D.Woolard, K. Petrus, Van Der Horst M. (2000) ISSN 0378- 4738-Water SA **26**:531
12. G. Baldwin, P.E. Rushbrook, C.G.Dent(1982) The testing of hazardous waste to assess their suitability for landfill disposal. Harwell report, AERE-R10737, November 1982
13. C. C. Wiles, "Standard Handbook of Hazardous Waste Treatment and Disposal." McGraw Hills, New York 7 (1988).
14. S. Saba, and A. Jamal, *Rasayan J. Chem*, **11(1)**,74(2018), DOI: [10.7324/RJC.2018.1111957](https://doi.org/10.7324/RJC.2018.1111957)
15. H .Akbar. , G. Krishan, S. D. Prajapati and Rakesh Saini, *Rasayan J. Chem.*, **9(1)**, 27 (2016)
16. J. L. Provis , R. J .Myers , C.E White ,V. Rose , J.S.J van Deventer , *Cem.Concr. Res.*, **42(6)**, 855 (2012), DOI: [10.1016/j.cemconres.2012.03.004](https://doi.org/10.1016/j.cemconres.2012.03.004)
17. P.S Deb, P.Nath, and P.K. Sarker, *Materials & Design* (1980-2015) **62**, 32 (2014), DOI: [10.1016/j.matdes.2014.05.001](https://doi.org/10.1016/j.matdes.2014.05.001)
18. G. Rajagopalan , C. Komarasamy , *Materiali in tehnologije / Materials and technology*, **50 (6)**, 929 (2016), DOI: [10.17222/mit.2015.230](https://doi.org/10.17222/mit.2015.230)
19. Gandhimathi, *Rasayan J. Chem.*, **10(2)**, 600 (2017), DOI: [10.7324/RJC.2017.1021677](https://doi.org/10.7324/RJC.2017.1021677)
20. M. Kavisri, P. Senthikumar , M. S. Gurukumar and Karunian J. Pushparaj, *Rasayan J. Chem.*, **11(1)**, 111 (2018), DOI: [10.7324/RJC.2018.1111805](https://doi.org/10.7324/RJC.2018.1111805)
21. T. Bakharev, *Cement and Concrete Research*, **35(6)**, 1224(2005), DOI: [10.1016/j.cemconres.2004.06.031](https://doi.org/10.1016/j.cemconres.2004.06.031)
22. P. Chindaprasirt, T. Chareerat, and V.Sirivivatnanon, *Cement and Concrete Composites* **29(3)**, 224 (2007), DOI: [10.1016/j.cemconcomp.2006.11.002](https://doi.org/10.1016/j.cemconcomp.2006.11.002)
23. R.N. Thakur, and S. Ghosh, *ARPN Journal of Engineering and Applied Sciences*, **4(4)**, 68(2009)
24. I. Idawati et al., *Cement and Concrete Composites*, **45**, 125(2014), DOI: [10.1016/j.cemconcomp.2013.09.006](https://doi.org/10.1016/j.cemconcomp.2013.09.006)
25. J. E. Oh, et al., *Cement and Concrete Research*, **40(2)**,189(2010), DOI: [10.1016/j.cemconres.2009.10.010](https://doi.org/10.1016/j.cemconres.2009.10.010)
26. S. Kumar, R. Kumar, and S. P. Mehrotra. *Journal of Materials Science*, **45(3)**,607 (2010), DOI: [10.1007/s10853-009-3934-5](https://doi.org/10.1007/s10853-009-3934-5)
27. R.R. Lloyd, *The Durability of Inorganic Polymer Cements*, PhD Thesis. University of Melbourne; 2008.
28. C.D. Woolard, K .Petrus, M .Van Der Horst (2000) ISSN 0378- 4738-Water SA **26**:531
29. S. Puligilla ,P. Mondal , *Cem. Concr. Res.*, **43**, 70 (2013), DOI: [10.1016/j.cemconres.2012.10.004](https://doi.org/10.1016/j.cemconres.2012.10.004)

30. J. L. Provis ,R.J. Myers ,C.E. White, V. Rose, J.S.J. van Deventer, *Cem. Concr. Res.*,**42(6)**, 855(2012), [DOI:10.1016/j.cemconres.2012.03.004](https://doi.org/10.1016/j.cemconres.2012.03.004)
31. T. Yang, X. Yao, Z. Zhang, H. Wang, *J. Sust. Cem. Based Mater.*, **1(4)**, 167(2012), [DOI:10.1080/21650373.2012.752621](https://doi.org/10.1080/21650373.2012.752621)
32. S. Thokchom, P. Ghosh, and S. Ghosh, *ARPJ. Eng. Appl. Sci* **4.1**: 65 (2009)
33. S. Thokchom, P. Ghosh, and S. Ghosh, *Journal of Civil Engineering and Management* ,**17(3)**, 393 (2011), [DOI:10.3846/13923730.2011.594225](https://doi.org/10.3846/13923730.2011.594225)
34. D. L. Y.Kong and J.G. Sanjayan, *Cement and Concrete Research*, **40(2)**, 334 (2010), [DOI:10.1016/j.cemconres.2009.10.017](https://doi.org/10.1016/j.cemconres.2009.10.017)
35. Z. Li, and L. Sifeng, *Journal of Materials in Civil Engineering*, **19(6)**, 470 (2007), [DOI:10.1061/\(ASCE\)0899-1561\(2007\)19:6\(470\)](https://doi.org/10.1061/(ASCE)0899-1561(2007)19:6(470))
36. C.K. Yip, G.C. Lukey, J.L. Provis, J.S.J. van Deventer, *Cem. Concr. Res.*, **38(4)**, 554 (2008), [DOI:10.1016/j.cemconres.2007.11.001](https://doi.org/10.1016/j.cemconres.2007.11.001)
37. C.K. Yip, G.C. Lukey, J.S.J. van Deventer, *Cem. Concr. Res.*, **35(9)**, 1688(2005), [DOI:10.1016/j.cemconres.2004.10.042](https://doi.org/10.1016/j.cemconres.2004.10.042)
38. I. García-Lodeiro, A. Palomo, A. Fernández-Jiménez, D.E. Macphee, *Cem. Concr. Res.*, **41(2)**, 923 (2011), [DOI:10.1016/j.cemconres.2011.05.006](https://doi.org/10.1016/j.cemconres.2011.05.006)
39. N. Marjanović, M. Komljenović, Z. Bašćarević, V. Nikolić, R. Petrović, *Ceramics International*, **41(1)**,1421 (2015), [DOI:10.1016/j.ceramint.2014.09.075](https://doi.org/10.1016/j.ceramint.2014.09.075)
40. A. Wardhono, D. W. Law, A. Strano, *Procedia Eng.*, **125**, 650(2015), [DOI:10.1016/j.proeng.2015.11.095](https://doi.org/10.1016/j.proeng.2015.11.095)
41. Z.Zhang,J.L.Provis,A.Reid,H.Wang,*Cem.Concr.Compos.*,**62**,97(2015),[DOI:10.1016/j.cemconcomp.2015.03.013](https://doi.org/10.1016/j.cemconcomp.2015.03.013)
42. P. Duxson, and J.L. Provis. *Journal of the American Ceramic Society*, **91(12)**, 3864(2008), [DOI:10.1111/j.1551-2916.2008.02787.x](https://doi.org/10.1111/j.1551-2916.2008.02787.x)
43. F. Collins, J. G. Sanjayan, *Cement and Concrete Research*, **30(9)**, 1401(2000), [DOI:10.1016/j.cemconres.2007.08.021](https://doi.org/10.1016/j.cemconres.2007.08.021)
44. D. L. Y. Kong, J.G. Sanjayan, and K. Sagoe-Crentsil, *Cement and Concrete Research* **37.12**: 1583(2007), [DOI:10.1016/j.cemconres.2007.08.021](https://doi.org/10.1016/j.cemconres.2007.08.021)
45. I. Ismail, S. A Bernal, J. L. Provis, S. Hamdan, J.S van Deventer, *Materials and structures*, **46.3**: 361 (2013), [DOI:10.1617/s11527-012-9906-2](https://doi.org/10.1617/s11527-012-9906-2)

[RJC-2036/2017]